Accepted Manuscript

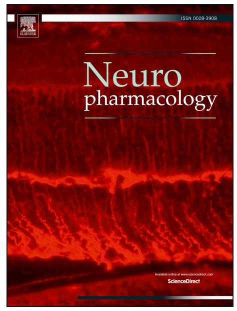

Effects of natural and synthetic isothiocyanate-based H_2S-releasers against chemotherapy-induced neuropathic pain: Role of Kv7 potassium channels

Lorenzo Di Cesare Mannelli, Elena Lucarini, Laura Micheli, Ilaria Mosca, Paolo Ambrosino, Maria Virginia Soldovieri, Alma Martelli, Lara Testai, Maurizio Taglialatela, Vincenzo Calderone, Carla Ghelardini

PII: S0028-3908(17)30179-X

DOI: 10.1016/j.neuropharm.2017.04.029

Reference: NP 6685

To appear in: *Neuropharmacology*

Received Date: 24 December 2016

Revised Date: 21 March 2017

Accepted Date: 17 April 2017

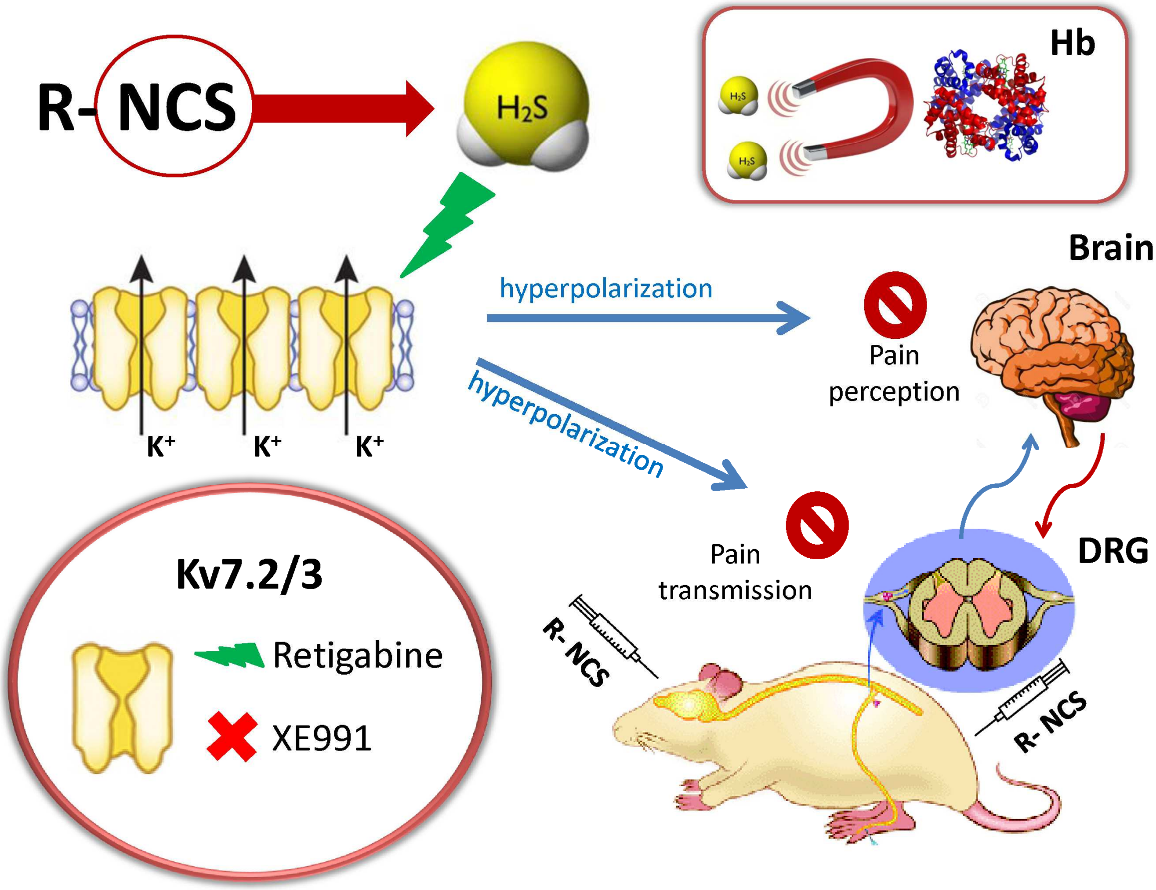
R- NCS
H2S
Hb
H2S
H2S
Brain
hyperpolarization
Pain
perception
hyperpolarization
K+
K+
K+
Pain
transmission
DRG
Kv7.2/3
Retigabine
XE991
R- NCS
R- NCS

Effects of natural and synthetic isothiocyanate-based H_2S-releasers against chemotherapy-induced neuropathic pain: role of Kv7 potassium channels

Lorenzo Di Cesare Mannelli[a], Elena Lucarini[a], Laura Micheli[a], Ilaria Mosca[b], Paolo Ambrosino[b], Maria Virginia Soldovieri[b], Alma Martelli[c], Lara Testai[c], Maurizio Taglialatela[b,d], Vincenzo Calderone[c], Carla Ghelardini[a]

[1]Dept. of Neuroscience, Psychology, Drug Research and Child Health - Neurofarba - Pharmacology and Toxicology Section, University of Florence, Viale pieraccini 6, Florence, Italy.

[2]Dept. of Medicine and Health Science, University of Molise, Via Francesco De Sanctis, 1 Campobasso, Italy.

[3]Dept. of Pharmacy, University of Pisa. Via Bonanno 6, Pisa, Italy.

[4]Section of Pharmacology; Department of Neuroscience, University of Naples Federico II, Via Pansini 5, Naples, Italy.

Corresponding author: Lorenzo Di Cesare Mannelli, Dept. of Neuroscience, Psychology, Drug Research and Child Health - Neurofarba - Pharmacology and Toxicology Section, University of Florence, Viale Pieraccini 6, 50139, Florence, Italy - lorenzo.mannelli@unifi.it

Abstract

Hydrogen sulfide (H_2S) is a crucial signaling molecule involved in several physiological and pathological processes. Nonetheless, the role of this gasotransmitter in the pathogenesis and treatment of neuropathic pain is controversial.

The aim of the present study was to investigate the pain relieving profile of a series of slow releasing H_2S donors (the natural allyl-isothiocyanate and the synthetics phenyl- and carboxyphenyl-isothiocyanate) in animal models of neuropathic pain induced by paclitaxel or oxaliplatin, anticancer drugs characterized by a dose-limiting neurotoxicity. The potential contribution of Kv7 potassium channels modulation was also studied.

Mice were treated with paclitaxel (2.0 mg kg^{-1}) i.p. on days 1, 3, 5 and 7; oxaliplatin (2.4 mg kg^{-1}) was administered i.p. on days 1-2, 5-9, 12-14. Behavioral tests were performed on day 15. In both models, single subcutaneous administrations of H_2S donors (1.33, 4.43, 13.31 μmol kg^{-1}) reduced the hypersensitivity to cold non-noxious stimuli (allodynia-related measurement). The prototypical H_2S donor NaHS was also effective. Activity was maintained after i.c.v. administrations. On the contrary, the S-lacking molecule allyl-isocyanate did not increase pain threshold; the H_2S-binding molecule hemoglobin abolished the pain-relieving effects of isothiocyanates and NaHS. The anti-neuropathic properties of H_2S donors were reverted by the Kv7 potassium channel blocker XE991. Currents carried by Kv7.2 homomers and Kv7.2/Kv7.3 heteromers expressed in CHO cells were potentiated by H_2S donors.

Sistemically- or centrally-administered isothiocyanates reduced chemotherapy-induced neuropathic pain by releasing H_2S. Activation of Kv7 channels largely mediate the anti-neuropathic effect.

Keywords: chemotherapy-induced neuropathic pain; H_2S donors; Kv7 channels; isothiocyanate; retigabine

Abbreviations: A-ITC, allyl isothiocyanate; A-IC, allyl isocyanate; CAT, cysteine aminotransferase; CBS, cystathionine-β-synthase; CMC, carboxymethyl cellulose; CO, carbon monoxide; CP-ITC, 3-carboxyphenyl isothiocyanate; CSE, cystathionine-γ-lyase; Hb, hemoglobin; H_2S, hydrogen sulphide; 3MST, 3-mercaptopyruvate sulfurtransferase; NaHS, sodium hydrosulfide hydrate; NO, nitric oxide; PEG, polyethylene glycol; P-ITC, phenyl isothiocyanate; TEA, tetraethylammonium.

1. Introduction

H_2S is historically known as a natural chemical hazard. Nowadays H_2S is considered a gasotransmitter in the mammalian body, like NO and CO, contributing to many physiological and pathological processes (Wang, 2002). It is endogenously produced mostly from L-cysteine and homocysteine through CSE, CBS and by a third pathway catalyzed by 3MST along with CAT (Shibuya et al. 2009). H_2S can also be generated by sulfate-reducing bacteria in the intestinal lumen (Roediger et al., 1997). CBS is preferentially expressed in the hippocampus and cerebellum (Abe and Kimura, 1996), mainly localized in astrocytes and microglial cells (Enokido et al., 2005). Despite the high level of CSE in the cardiovascular system, the enzyme was also found in the nervous tissue in microglial cells (Lee et al., 2006) and in spinal cord- (Distrutti et al., 2006) and cerebellar granule-neurons (Garcia-Bereguiain et al., 2008). Also 3MST is present in neurons and astrocytes (Shibuya et al., 2009; Zhao et al., 2013).

In the nervous system, H_2S is involved in synaptic modulation by interacting with ion channels, second messengers and modifying sulfhydryl groups of proteins (Wallace and Wang, 2015). A major role in redox balance, mitochondrial bioenergetics, apoptosis and inflammatory processes (Kamat et al., 2015) leads to H_2S relevance in memory, cognition and learning (Nagpure and Bian, 2015) as well as in neuroprotection (Paul and Snyder, 2015).

The role of H_2S in pain modulation is controversial: conflicting data suggest that it is both pronociceptive (mainly through Cav3.2 T-type Ca^{2+} channels and transient receptor potential ankyrin 1 – TRPA1 channels; Terada and Kawabata, 2015) and anti-nociceptive (Wallace and Wang, 2015) depending on the models used and the types and doses of H_2S donors or modulators used. Nonetheless, several studies have suggested significant pain relieving effects of H_2S donors against neuropathic and visceral pain (Distrutti et al., 2006; Lin et al., 2014; Kida et al., 2015). Recently, some isothiocyanate derivatives, slow releasing H_2S-donor moieties, and NaHS, a prototypical H_2S-generating agent, were described as activators of Kv7 potassium channels (Testai et al., 2016; Martelli et al., 2013a), a class of the voltage-gated potassium channels which plays a pivotal role in pain modulation (Zheng et al., 2013; Busserolles et al., 2016). A decreased expression of Kv7 channels contributes to neuropathic hyperalgesia (Rose et al., 2011) since channel activation inhibits C and Aδ fiber-mediated responses of dorsal horn neurons (Passmore et al., 2003) and reduces the ectopic generation of action potentials in neuropathic pain (Lang et al., 2008). On these premises, Kv7 channel activators like retigabine are currently regarded as anti-hyperalgesic compounds (Nodera et al., 2011; Blackburn-Munro and Jensen, 2003).

Aim of the present work was to investigate the pharmacological profile of different isothiocyanates (the chemical structures are depicted in Scheme 1), after acute subcutaneous administration in mouse models of chemotherapy-induced neuropathic pain evoked by paclitaxel and oxaliplatin (Di Cesare Mannelli et al., 2013; Fariello et al., 2014). In particular, allyl isothiocyanate, naturally occurring in many species of Brassicaceae (Citi et al., 2014), and the synthetic phenyl- and carboxyphenyl isothiocyanate were compared with NaHS. The pharmacodynamic involvement of H_2S and Kv7 was studied.

2. Methods

2.1. Animals

Male CD-1 albino mice (Envigo, Varese, Italy) weighing approximately 22–25 g at the beginning of the experimental procedure, were used. Animals were housed in CeSAL (Centro Stabulazione Animali da Laboratorio, University of Florence) and used at least 1 week after their arrival. Ten mice were housed per cage (size 26 × 41 cm); animals were fed a standard laboratory diet and tap water *ad libitum*, and kept at 23 ± 1 °C with a 12 h light/dark cycle, light at 7 a.m. All animal manipulations were carried out according to the Directive 2010/63/EU of the European parliament and of the European Union council (22 September 2010) on the protection of animals used for scientific purposes. The ethical policy of the University of Florence complies with the Guide for the Care and Use of Laboratory Animals of the US National Institutes of Health (NIH Publication No. 85-23, revised 1996; University of Florence assurance number: A5278-01). Formal approval to conduct the experiments described was obtained from the Animal Subjects Review Board of the University of Florence. Experiments involving animals have been reported according to ARRIVE guidelines (McGrath and Lilley, 2015). All efforts were made to minimize animal suffering and to reduce the number of animals used.

2.2. Paclitaxel- and oxaliplatin-induced neuropathic pain models

Mice treated with paclitaxel (2.0 mg kg^{-1}) were injected i.p. on four alternate days (days 1, 3, 5 and 7) (Polomano and Bennett., 2001). Paclitaxel was dissolved in a mixture of 10% saline solution and Cremophor EL, a derivative of castor oil and ethylene oxide that is clinically used as paclitaxel vehicle. Mice treated with oxaliplatin (2.4 mg kg^{-1}) were administered i.p. on days 1-2, 5-9, 12-14 (10 i.p. injections) (Cavaletti et al., 2001). Oxaliplatin was dissolved in 5% glucose solution. Control animals received an equivalent volume of vehicle. Behavioral tests were performed on day 15.

2.3. Compound administrations and in vitro uses

A-ITC, A-IC, P-ITC (Sigma-Aldrich, Milan, Italy) and CP-ITC (Fluorochem Ltd, Hadfield, UK) were dissolved in saline solution with 0.5% PEG. GYY4137 dichloromethane complex and NaHS (Sigma-Aldrich, Milan, Italy) were dissolved in saline solution. Morphine (S.A.L.A.R.S., Como, Italy) and pregabalin (3B Scientific Corporation, China) were dissolved in saline solution. Celecoxib (Sigma-Aldrich, Italy) and duloxetine (Sequoia Research, UK) were dissolved in 1% CMC. Compounds were acutely administered as follows. The doses of NaHS were chosen on the bases of previously published H_2S releasing and antinociceptive properties (Distrutti et al., 2006; Martelli et al., 2013b) (1.33, 4.43, 13.31 and 38 μmol kg^{-1} corresponding to 0.1, 0.33, 1 and 3 mg kg^{-1} were administered by s.c. route or 4.43 nmol/mouse by i.c.v. route); P-ITC (1.33, 4.43 and 13.31 μmol kg^{-1} s.c. or 4.43 nmol/mouse i.c.v.); CP-ITC, A-ITC and A-IC (1.33, 4.43 and 13.31 μmol kg^{-1} s.c.); GYY4137 (4.43 μmol kg^{-1} s.c.). As reference compounds were used morphine (21.75 μmol kg^{-1}; 7 mg kg^{-1} s.c.; Rashid et al., 2004), pregabalin (94.20 μmol kg^{-1}; 15 mg kg^{-1} s.c.; Di Cesare Mannelli et al., 2015a), celecoxib (104.88 μmol kg^{-1}; 40 mg kg^{-1} p.o.; Jiang et al., 2016) and duloxetine (50.43 μmol kg^{-1}; 15 mg kg^{-1} p.o.; Di Cesare Mannelli et al., 2014). In additional experiment P-ITC, NaHS and GYY4137 (4.43 μmol kg^{-1}) were administered s.c. in mixture with 3.10 μmol kg^{-1} (200 mg kg^{-1}) human Hb (Sigma-Aldrich, Italy) in saline solution and behavioral tests were carried out after 15, 30, 45 and 60 min from injection. The Kv7 potassium channel blocker XE991 (Tocris Bioscience, Italy; 2.66 μmol kg^{-1}; 1 mg kg^{-1}; Blackburn-Munro and Jensen, 2003) was dissolved in saline solution and administered i.p. 15 min before the injection of tested compounds. The Kv7 potassium channel opener retigabine (Sequoia Research, UK; 65.93 μmol kg^{-1}; 20 mg kg^{-1}; Blackburn-Munro and Jensen, 2003; Miceli et al., 2008) was dissolved in 1% CMC and administered p.o..

In electrophysiological measurements, retigabine (Valeant Pharmaceuticals, USA) and CP-ITC were dissolved in DMSO, whereas NaHS (Sigma-Aldrich, Italy) was dissolved in water. In each experiment, the same volume of solvent present in the drug solution was added to the control solution; maximal concentration of DMSO (0.1%) was *per se* ineffective. A-ITC, A-IC and P-ITC are liquid at room temperature, thus requiring no solvent addition in the respective control solution. Fresh drug stocks (at M concentration) were prepared daily or, as in the case of NaHS, twice daily. Fast solution exchanges (<1 s) were achieved, as previously reported (Ambrosino et al., 2015), by means of a cFlow 8 flow controller attached to a cF-8VS 8-valve switching apparatus and a MPRE8 miniature flow outlet having an inside diameter of 360 μm and a mixing volume at the tip of 1-2 μl (Cell Microcontrols, Norfolk, VA, USA) positioned within 200 μm of the cell.

2.4. Cold Plate Test

The animals were placed in a stainless steel box (12 cm × 20 cm × 10 cm) with a cold plate as floor. The temperature of the cold plate was kept constant at 4°C ± 1°C. Pain-related behavior (licking of the hind paw) was observed and the time (seconds) of the first sign was recorded. The cut-off time of the latency of paw lifting or licking was set at 60 seconds (Di Cesare Mannelli et al., 2013).

2.5. Von Frey test

Animals were placed in 10 cm × 10 cm Plexiglas boxes equipped with a metallic mesh floor, 20 cm above the bench. Animals were allowed to habituate themselves to their environment for 15 min before the test. An electronic Von Frey hair unit (Ugo Basile, Varese, Italy) was used: the withdrawal threshold was evaluated by applying forces ranging from 0 to 5 g with 0.2 g accuracy. Punctuate stimulus was delivered to the mid-plantar area of each posterior paw from below the mesh floor through a plastic tip and the withdrawal threshold was automatically displayed on the screen. The paw sensitivity threshold was defined as the minimum force required to elicit a robust and immediate withdrawal reflex of the paw. Voluntary movements associated with locomotion were not considered as a withdrawal response. Stimuli were applied to each anterior paw at 5 s intervals. Measurements were repeated 5 times and the final value was obtained by averaging the 5 measurements (Ta et al., 2009).

2.6. Hot-plate test

Hot-plate test was carried out accordingly with O'Callaghan and Holzman (1975). Mice were placed inside a stainless steel container, thermostatically set at 52.5 ± 0.1 °C in a precision water-bath from KW Mechanical Workshop, Siena, Italy. Reaction times (s) were measured with a stop-watch before and at regular intervals up to a maximum of 60 min after treatment. The end point used was the licking of the fore or hind paws. Before treating animals tested compounds, a pretest was performed: those mice scoring below 12 and over 18 s were rejected. An arbitrary cutoff time of 45 s was adopted.

2.7. Cell culture and transfection

As previously described (Miceli et al., 2013), CHO cells were grown in DMEM medium supplemented with 10% FBS, 100 U mL^{-1} penicillin/streptomycin and 2 mM L-glutamine. The cells were kept in a humidified atmosphere at 37°C with 5% CO_2 in 100 mm plastic Petri dishes. Twenty-four hours after plating on 35-mm glass coverslips (Carolina Biological Supply Co., Burlington, NC) coated with poly-L-lysine (Sigma, Milan, Italy), CHO cells were transiently transfected using Lipofectamine 2000 (Invitrogen, Milan, Italy), according to the manufacturer protocols, with plasmids containing the cDNAs encoding for Kv7.2 or Kv7.2 and Kv7.3 (cDNA transfection ratio 1:1) and for the Enhanced Green Fluorescent Protein (Clontech, Palo Alto, CA; 1/10 of the total cDNA), used as a transfection marker.

2.8. Patch-clamp electrophysiology

Currents from CHO cells were recorded at room temperature (20-22 °C) 1 day after transfection by using an Axopatch 200A (Molecular Devices) and the whole-cell configuration of the patch-clamp technique, with glass micropipettes of 3 to 5 MΩ resistance, as previously described (Ambrosino et al., 2015). The extracellular solution contained (in mM) 138 NaCl, 2 $CaCl_2$, 5.4 KCl, 1 $MgCl_2$, 10 glucose, and 10 Hepes, pH 7.4 adjusted with NaOH; the pipette (intracellular) solution contained (in mM) 140 KCl, 2 $MgCl_2$, 10 EGTA, 10 Hepes, 5 Mg-ATP, pH 7.3 to 7.4 adjusted with KOH. pCLAMP software (version 10.0.2) was used for data acquisition and analysis. Linear cell capacitance (C) was determined by integrating the area under the whole-cell capacity transient, evoked by short (5-10 ms) pulses from -80 to -75 mV with the whole-cell capacitance compensation circuit of the Axopatch 200A turned off. Currents were activated by 3-s voltage ramps from -80 mV to 0 mV at 0.1-Hz frequency. Current densities (expressed in pA/pF) were calculated by dividing currents at 0 mV by C. Currents were corrected offline for leakage currents using standard subtraction routines (Clampfit module of pClamp 10). In analogy to the reported effects of the prototypical Kv7 activator retigabine (Miceli et al., 2008), two parameters were used to quantify drug-induced effects: the percent of current potentiation at 0 mV, and the leftward shift of the membrane potential at which currents measured during drug application were identical to those recorded in control solution at -40 mV (Miceli et al., 2013); this latter parameter was arbitrarily defined as ΔV_{-40}. Both parameters were determined after 1-2-min drug application, a time sufficient for drug-induced effects to reach steady-state. Current activation and deactivation kinetics were analyzed by fitting the current traces to a single or to a double-exponential function of the following form: $y = amp_f\ \exp(-t/\tau_f) + amps\ \exp(-t/\tau_s)$, where amp_f and amp_s indicate the amplitude of the fast and slow exponential components respectively, whereas τ_f and τ_s indicate the time constants of these components, as previously described (Soldovieri et al., 2007).

2.9. Statistical analysis

Behavioral measurements were performed on 16 mice for each treatment carried out in 2 different experimental sets. Results were expressed as mean ± S.E.M. The analysis of variance of behavioral data was performed by one way ANOVA, a Bonferroni's significant difference procedure was used as post-hoc comparison. *P* values of less than 0.05 or 0.01 were considered significant. Statistically significant differences in electrophysiology data were evaluated with the Student t test, or with ANOVA followed by the Student-Newman-Keuls test when multiple groups were compared, with the threshold set at $P<0.05$. Investigators were blind to all experimental procedures. Data were analyzed using the "Origin 9" software (OriginLab, Northampton, USA). The area under the curve (AUC) of the antinociceptive effects was calculated using the same software, evaluating the data from 0–60 min.

3. Results

3.1. Behavioral studies

On day 15, paclitaxel-treated mice showed a significantly decreased latency to pain-related behaviors induced by a cold stimulus (11.5 ± 0.9 s) compared to control mice (23.4 ± 1.7 s) treated with vehicle (Figure 1). The effect of single administration s.c. of three different doses of P-ITC, CP-ITC, A-ITC and NaHS on paclitaxel-treated mice is shown in Figure 1a, b, c and d, respectively. P-ITC is active starting from 4.43 μmol kg^{-1}. The dose of 13.31 μmol kg^{-1} was significant starting 15 min after administration, the effect lasted until 45 min. CP-ITC (1.33 μmol kg^{-1}) increased pain threshold only 15 min after administration. Otherwise, 4.43 μmol kg^{-1} and 13.31 μmol kg^{-1} CP-ITC increased the licking latency long lastingly. A-ITC (4.43 and 13.31 μmol kg^{-1}) was active between 15 and 45 min after administration. NaHS was active in paclitaxel-treated mice starting from the dose of 4.43 μmol kg^{-1}, plateauing between 30 min and 45 min after administration. The highest dose was lesser effective.

The pain threshold measurements of oxaliplatin-treated animals (Cold plate test) is shown in Figure 2. On day 15, oxaliplatin decreased the licking latency to 12.6 ± 0.7 s in comparison to control mice (21.5 ± 1.2 s). The lower dose of P-ITC induced a slight effect whereas 4.43 μmol kg^{-1} and 13.31 μmol kg^{-1} significantly increased the licking latency starting 15 min after administration and reaching a maximum effect 30 min after administration. CP-ITC (1.31 μmol kg^{-1}) improved pain threshold between 15 and 30 min. Oxaliplatin-induced hypersensitivity was fully abolished by the high doses of CP-ITC (4.43 μmol kg^{-1} and 13.31 μmol kg^{-1}). NaHS (13.31 μmol kg^{-1}) was effective between 15 and 45 min. The higher dose was lesser long-lasting. Morphine (21.75 μmol kg^{-1} s.c.) did not increase the licking latency of oxaliplatin-treated mice. Celecoxib (104.88 μmol kg^{-1} p.o.) and pregabalin (94.20 μmol kg^{-1} s.c.) significantly increased pain threshold only 15 min after administration. Duloxetine (50.43 μmol kg^{-1} p.o.) induced a maximum effect 30 min after administration (Figure 2). Effects of these reference compounds on paclitaxel-induced neuropathic pain are already published. In particular, pregabalin and duloxetin showed similar efficacy than in oxaliplatin model (Ito et al., 2012); on the contrary, morphine (Xu et al., 2011) was partially active against paclitaxel (differently from oxaliplatin) whereas celecoxib did not (Ito et al., 2012).

P-ITC, CP-ITC and NaHS showed similar efficacy against paclitaxel- and oxaliplatin-dependent hypersensitivity when evoked by mechanical stimulus (Von Frey test, Supplementary Figure S1 and S2).

Figure 3a shows the comparison between the responses to acute administration s.c. of A-ITC and A-IC on oxaliplatin-treated mice. A-ITC (13.31 μmol kg^{-1}) increased licking latency up to control level. On the contrary, A-IC, the analogue molecule without the sulfhydryl group (Scheme 1), was not active after administration s.c. of the same dosage. In Figure 3b, the enhancement of pain threshold induced by a single administration of NaHS (13.31 μmol kg^{-1}), P-ITC (4.43 μmol kg^{-1}), CP-ITC (4.43 μmol kg^{-1}), A-ITC (4.43 μmol kg^{-1}) expressed as AUC (0 – 60 min) is shown in comparison to oxaliplatin-treated mice. The H_2S-binding molecule Hb (3.1 μmol kg^{-1} s.c.), co-administered with the H_2S donors, was able to fully prevent the anti-hypersensitive efficacy. Hb *per se* was ineffective (Figure 3b). Similar results were obtained by the non-isothiocyanate H_2S donors GYY4137 (4.43 μmol kg^{-1} s.c.; GYY) (Figure 3b). In the Supplementary Figure S3, effects over time of this morpholine-derivative were shown in the absence and in the presence of Hb.

Pain relieving activity of NaHS (13.31 μmol kg^{-1} s.c.), P-ITC, CP-ITC and A-ITC (all at 4.43 μmol kg^{-1} s.c.) was fully prevented by the administration i.p. of the Kv7 potassium channel blocker XE991 (2.66 μmol kg^{-1}) as shown in Figure 4a (AUC values; 0 – 60 min). The relevance of Kv7 in pain modulation was confirmed through the effectiveness showed by the Kv7 opener retigabine (65.93 μmol kg^{-1} p.o.) in oxaliplatin-treated mice (Figure 4b). XE991 reverted retigabine efficacy without altering the pain threshold *per se* (Figure 4b). A dose-response curve of XE-991 *per se* effects on oxaliplatin-induced hypersensitivity is shown in the Supplementary Figure S4.

To evaluate the central component of the anti-neuropathic effect of H_2S donor molecules, the efficacy of NaHS (13.31 nmol/mouse) and P-ITC (4.43 nmol/mouse) was evaluated after i.c.v. administration in oxaliplatin-treated mice (Figure 4c). Both compounds increased the pain threshold up to control group levels peaking 30 min after administration. These effects were fully prevented by the pre-administration of XE991 i.p. (Figure 4c).

Neither NaHS (13.31 μmol kg^{-1} s.c.) nor A-ITC and P-ITC (both 4.43 μmol kg^{-1} s.c.) were able to influence the normal pain threshold of naïve animals as evaluated by Hot plate test using a thermal noxious stimulus able to highlight analgesic effects (Supplementary Figure S5).

3.2. Electrophysiological studies

Given the *in vivo* data showing that the Kv7 channel blocker XE991 antagonized the pain-relieving activity of H_2S donors, the ability of these drugs to directly influence the activity of Kv7 channels involved in pain information processing was also investigated. To this aim, patch-clamp experiments in CHO cells transfected with Kv7.2 and Kv7.3 cDNAs were carried out. In response to voltage ramps from -80 mV to 0 mV, heteromeric channels formed by Kv7.2/3 subunits elicit robust voltage-dependent, outwardly rectifying K^+ currents. Perfusion for 1-2 min with the Kv7 opener retigabine (0.01 mM) led to an increase in maximal current of ~ 2-fold, and to a leftward shift in the threshold potential of current activation of ~ -20 mV (Figure 5). Using an identical experimental paradigm, perfusion with NaHS (0.01-10 mM), A-ITC (0.01-10 mM), P-ITC (1-100 mM), or CP-ITC (0.01-10 mM) dose-dependently increased maximal current size at 0 mV (Figure 5a and 5b) and shifted the ΔV_{-40} toward more negative membrane potential values (Figure 5a and 5c); notably, the effect of CP-ITC on ΔV_{-40}, although smaller than that observed with retigabine, was significantly greater than that of NaHS. By contrast, no effect was observed upon perfusion with 1-10 mM A-IC, suggesting that the presence of a thiol group was essential for the functional effects observed on Kv7 currents by A-ITC (Scheme 1). Finally, CP-ITC appeared more efficacious and potent than P-ITC in potentiating Kv7.2/3 maximal currents and negatively-shifting the ΔV_{-40}; this latter result is consistent with the higher H_2S levels produced by CP-ITC when compared to P-ITC, thus highlighting a relevant role for the carboxyl group in this process (Martelli et al., 2014).

K^+ currents carried by Kv7.2/3 channels displayed activation kinetics which could be fitted by a sum of two exponential functions (Wang et al., 1998; Castaldo et al., 2002), with a fast and a slow time constants (τ_f and τ_s, respectively) (Supplementary Figure S6, panels a and b); at any given potential above -40 mV, the relative amplitude of the fast component, called A_f, largely dominated over that of the slow component, called A_s; thus, the ratio of A_f and A_s, expressed as $A_f/(A_f+A_s)$, was around 1 at all potentials investigated (Supplementary Figure S6, panel c). Perfusion with 1 mM CP-ITC failed to modify current activation rates, as no change was detected in either τf or τs before and after drug exposure at any given potential between -40 mV to +40mV. On the other hand, the H2S donor significantly decreased the ratio between the two components (described by Af/Af+As) for potentials ≥ -20 mV; this was due to a drug-dependent increase in the absolute amplitude of the slow component, virtually absent in control conditions. Perfusion with 1 mM CP-ITC also markedly reduced current deactivation kinetics (Supplementary Figure S6, panels d and e). In rat hippocampal presynaptic terminals (Martire et al., 2004) and in large fibers of the rat sciatic nerve (Schwarz et al., 2006), functional Kv7.2 homomers have also been described; when compared to heteromeric Kv7.2/3 channels, Kv7.2 currents are 4-6 times smaller, activate at slightly more positive membrane voltages (Wang et al., 1998), and display a higher sensitivity to the pore blocker TEA (Hadley et al., 2000). To investigate whether H_2S donors differentially affected Kv7.2 homomers when compared to Kv7.2/3 heteromers, electrophysiological experiments were also carried out in CHO cells transfected only with Kv7.2 cDNA. As shown in Supplementary Figure S7, Kv7.2 currents showed a pharmacological profile very similar to that of Kv7.2/3 currents, being potentiated (though with a lower potency and efficacy when compared to retigabine) by 1 mM NaHS, A-ITC, P-ITC, or CP-ITC, and being unaffected by 1 mM A-IC.

4. Discussion

The development of painful neuropathies is a severe dose-limiting side effect of commonly used chemotherapeutic agents including taxanes, vinca alkaloids and platinum agents (Ward et al., 2014; Watkins et al., 2005). Paclitaxel-induced neurotoxicity is characterized by numbness, tingling and burning pain (Dougherty et al., 2004); repeated oxaliplatin administrations induce a chronic neurological syndrome that persists between and after treatment (Beijers et al., 1999; Souglakos et al., 2002) negatively influencing patient's quality of life. The pharmacological management of chemotherapy-induced neuropathy remains largely ineffective (Hershman et al., 2014).

The present results show the pain relieving efficacy of novel isothiocyanate-based H_2S-donors, along with the well-known reference compounds NaHS and GYY4137, in animal models of neuropathic pain induced by anticancer drugs. P-ITC, CP-ITC and A-ITC reduce the hypersensitivity to a cold non-noxious stimulus (allodynia-related measurement) after the acute systemic administration of very low doses both in paclitaxel and oxaliplatin-treated animals (effectiveness has been demonstrated also using a mechanical non-noxious stimulus, both the responses are strictly related to the neuropathic condition; Di Cesare Mannelli et al. 2013) Because of the similar pharmacological profile shown in the two models, further experiments were carried out in the best characterized neuropathy model, namely that evoked by the platin derivative.

When compared to duloxetine and pregabalin, two molecules currently in clinical use to reduce the symptoms of chemotherapy-induced neuropathy (Hershman et al., 2014), isothiocyanates show similar efficacy at 10-times lower doses; morphine is ineffective against oxaliplatin-dependent pain. NaHS, a prototypical H_2S-donor, shows similar efficacy as isothiocyanates, despite being less potent. Both synthetic (Martelli et al. 2014) and naturally-occurring (Citi et al., 2014) isothiocyanates act as H_2S-releasing compounds, and our results are consistent with an involvement of this gasotransmitter in the antinociceptive effects shown by these molecules. The H_2S-binding molecule Hb (Pietri et al., 2011) fully prevented the anti-neuropathic efficacy of P-ITC, CP-ITC, A-ITC and NaHS, as well as of GYY4137, a morpholin-derivative able to slowly release H_2S both *in vitro* and *in vivo* (Li et al., 2008). Moreover, A-IC, the corresponding isocyanate of A-ITC, unable to release H_2S, was completely ineffective against oxaliplatin-induced neuropathy. Efficacy of P-ITC and NaHS was also measurable after i.c.v. administration, suggesting a central component of the H_2S donors-mediated anti-neuropathic property. Independently by the route of administration, these compounds were effective at very low doses. Characteristically, while some compounds like P-ITC and CP-ITC seem to reach a maximal effect beyond which the dose increase is not significant, the anti-neuropathic effects of the highest doses of NaHS and A-ITC were less evident when compared to lower doses. Although this bell-shaped dose-dependence possibly involves the complex pharmacokinetic profile of specific H_2S donors, it should be highlighted that a similar phenomenon has been also reported for the mitochondrial effects of H_2S. In fact, low concentrations of H_2S donors stimulate the mitochondrial electron transport, evoke protective effects maintaining mitochondrial function, protecting mitochondrial DNA integrity, and inhibiting mitochondrial protein oxidation (Ahmad et al., 2016). On the contrary, elevation of H_2S concentrations beyond a certain concentration range becomes cytotoxic, pro-oxidant, and suppresses mitochondrial electron transport (Szabo et al., 2014).

The lipid-soluble nature of H_2S enables this gasotransmitter to easily reach its molecular targets on the plasma membrane, inside the cytosol or in intracellular organelles. Its characteristic membrane permeability, together with its unique chemical reactivity with certain types of macromolecules in different types of cells, makes H_2S a pleiotropic and powerful signaling molecule (Wallace and Wang, 2015). Voltage-gated potassium channel subunits encoded by the Kv7 subfamily have been shown to mediate a large part of the H2S-induced cardiovascular effects through an effect on Kv7.4 subunits (Schleifenbaum et al., 2010; Martelli et al., 2013a). The Kv7 gene family includes five members (Kv7.1-5), each showing a specific tissue distribution and functional role (Soldovieri et al., 2011). In particular, heteromeric assembly of Kv7.2 and Kv7.3 subunits is believed to provide a major contribution to a sub-threshold slowly-activating and deactivating, and non-inactivating K^+ current known as the M-current (Wang et al., 1998), which limits repetitive firing and causes spike-frequency adaptation (Soldovieri et al., 2011). Heteromeric Kv7.2/3 channels appear as the main players in pain information processing, being abundantly expressed in nodes of Ranvier and the cell bodies of large sensory neurons as well as in the dorsal horns, the thalamus and the cortex (Wang and Li, 2016). Notably, although Kv7.5 subunits are also abundantly expressed in C-fibers and control excitability of nociceptive neurons (King and Scherer, 2012), the pharmacological profile of the M currents recorded from nociceptive DRG neurons speaks against a strong contribution of

Kv7.5 (Du and Gamper, 2013). Inhibition of Kv7 channels with XE-991, a specific and potent blocker of the currents carried by Kv7 channels (Wang et al., 1998), leads to hyperexcitability of primary sensory neurons (Zheng et al., 2013). On the other hand, retigabine, an activator of neuronal Kv7 channels (Miceli et al., 2008), was neuroprotective against cisplatin- (Nodera et al., 2011) and oxaliplatin- (Abd-Elsayed et al., 2015) induced neuropathy, decreased osteoarticular and neuropathic pain (Li et al., 2015; Brown and Passmore, 2009), and suppressed the excitability of nociceptive cold-sensing trigeminal ganglion neurons (Abd-Elsayed et al., 2015). Moreover, flupirtine, a retigabine-analogue also acting as a Kv7 activator (Martire et al., 2004) suppressed axonal hyperexcitability of peripheral nerve exposed to oxaliplatin (Sittl et al., 2010). All these evidence point toward a crucial role of Kv7 channels in several models of persistent pain. In the present study, retigabine is shown to effectively protect against oxaliplatin-dependent pain, and the Kv7 blocker XE991 fully counteracted the pain relieving effects of retigabine as well as of isothiocyanates and NaHS administered by both systemic or i.c.v. routes. Importantly, XE991 reverted H_2S donors effects at dosages that did not modify oxaliplatin-hypersensitivity *per se* (present data). Furthermore, XE991 did not show anti-nociceptive properties since it did not modify the normal pain threshold of naïve animals (Blackburn-Munro et al., 2003; Hayashi et al., 2014). These data led us to hypothesize that H_2S, by activating Kv7 channels, reduces neuronal hyperexcitability both in DRG and in central neurons, thus normalizing the altered electrophysiological activity occurring during chemotherapy-induced neuropathic pain (Di Cesare Mannelli et al., 2015b)

Patch-clamp experiments in CHO cells heterologously-expressing Kv7.2 and Kv7.3 cDNAs revealed that Kv7.2/3 heteromeric currents showed concentration-dependent activation by H_2S-releasing isothiocyanates, suggesting that these channels mediate at least some of the anti-hypersensitive effects exerted *in vivo* by these compounds. Biophysical analysis of the changes introduced by the most effective H2S donor herein investigated (CP-ITC) on Kv7.2/3 activation and deactivation kinetics are suggestive of a drug-induced increased stabilization of the open configuration of the channel, leading to a decreased rate of channel deactivation, and a facilitation of channel opening by voltage. The present experiments do not allow to discriminate whether H_2S activated Kv7.2/3 currents by interacting directly with the channel subunits or whether intermediate messengers are involved. It would be interesting to verify a possible interaction of H_2S with radical oxygen species (ROS), given the fact that H_2O_2 markedly increase currents formed by Kv7.2, Kv7.3, and Kv7.4 channels (Gamper et al. 2006). In Kv7.4 channels, a conserved cysteine triplet in the S2–S3 linker was identified as critical for this pharmacological effect; whether this same site is also involved in the described effects of H2S on Kv7.2 /3 channels is still unknown.

It should be noted that all the isothiocyanates used in this study, along with the reference H_2S donor NaHS, showed anti-neuropathic effects. However, they exhibited different degrees of efficacy and potency (in the *in vivo* experiments and in the electrophysiological studies), not clearly related with their H_2S-releasing profiles. Slow H_2S-donors, such as GYY4137, are often more effective than rapid donors, such as NaHS, suggesting that long-lasting generation of relatively lower concentrations of H_2S can be preferable for certain pharmacological effects (Li et al., 2008). Moreover, the isothiocyanates used in this study are not "spontaneous" H_2S-donors: indeed, the H_2S-release from these compounds is triggered by the presence of organic thiols such as L-cystein (Martelli et al., 2014). Thus, this process can be "smartly" promoted in biological environments by a large availability of endogenous organic thiols (and perhaps by other metabolic reactions), but can be also influenced by variables linked to different experimental models which can make difficult the quantitative correlation between H_2S-release and pharmacological effects. Finally, even pharmacokinetic aspects, concerning the ability of the H_2S-prodrugs to reach the pharmacological target, may play a role.

The emerging data on the biological effects of H_2S, and the etiopathogenetic roles of both excessive and defective H_2S biosynthesis in some diseases, support two main approaches for the development of sulfide-based therapeutics: suppression of endogenous sulfide formation by inhibitors of CSE and CBS, and gaseous H_2S or H_2S-releasing compounds (sulfide donors). The formers (DL-propargylglycine and β-cyanoalanine) have low potency and a questionable selectivity (Szabò, 2007). Concerning the latter compounds, excluding gaseous H_2S for its poor safety, H_2S equivalents or releasing agents (i.e. donors) are becoming important research tools (Zhao et al., 2014). In the past, some series of different H_2S pro-drugs were developed (Zheng et al., 2015; Zhao et al., 2014) often obtaining a limited control of gas release. Presently, there is still scarce heterogeneity of H_2S-releasing moieties endowed with satisfactory pharmacological and chemical (stability) features. Isothiocyanate exhibit interesting H_2S-releasing properties which can be usefully employed for therapeutic purposes. The effectiveness of allyl isothiocyanate, mainly obtained from the seeds of *Brassica nigra* L., raises the intriguing possibility to exploit the plant kingdom as a source of H_2S-based therapeutics against neuropathic pain.

In this perspective, the present study demonstrates that H_2S-releasing compounds, such as the "gold standard" GYY4137 or the novel isothiocyanates, promote H_2S-mediated activation of Kv7 channels and may represent an exciting and innovative approach to drug-resistant forms of pain such as chemotherapy-induced neuropathies.

Acknowledgments and funding sources

This work was supported by the Italian Ministry of Instruction, University and Research (MIUR) and by the University of Florence. Work in Dr. Taglialatela's lab is supported by Telethon (Grant number: GGP15113).

References

Abd-Elsayed, A.A., Ikeda, R., Jia, Z., Ling, J., Zuo, X., Li, M., et al., 2015. KCNQ channels in nociceptive cold-sensing trigeminal ganglion neurons as therapeutic targets for treating orofacial cold hyperalgesia. Mol. Pain. 11: 45.

Abe, K., Kimura, H., 1996. The possible role of hydrogen sulfide as an endogenous neuromodulator. J. Neurosci. 16: 1066-1071.

Ahmad, A., Olah, G., Szczesny, B., Wood, M.E., Whiteman, M., Szabo, C., 2016. AP39, a mitochondrially targeted hydrogen sulfide donor, exerts protective effects in renal epithelial cells subjected to oxidative stress in vitro and in acute renal injury in vivo. Shock 45: 88-97.

Ambrosino, P., Alaimo, A., Bartollino, S., Manocchio, L., De Maria, M., Mosca, I. et al., 2015. Epilepsy-causing mutations in Kv7.2 C-terminus affect binding and functional modulation by calmodulin. Biochim. Biophys. Acta 1852(9): 1856-1866.

Beijers, A.J.M., Mols, F., Vreugdenhil, G., 2014. A systematic review on chronic oxaliplatin-induced peripheral neuropathy and the relation with oxaliplatin administration. Support Care Cancer 22: 1999-2007.

Blackburn-Munro, G., Jensen, B.S., 2003. The anticonvulsant retigabine attenuates nociceptive behaviours in rat models of persistent and neuropathic pain. Eur. J. Pharmacol. 460(2): 109-116.

Brown, D.A., Passmore, G.M. 2009. Neural KCNQ (kv7) channels. Br. J. Pharmacol. 156: 1185-1195.

Busserolles, J., Tsantoulas, C., Eschalier, A., López, G.J., 2016. Potassium channels in neuropathic pain: advances, challenges, and emerging ideas. Pain 157 Suppl 1: S7-14.

Castaldo, P., Del Giudice, E.M., Coppola, G., Pascotto, A., Annunziato, L., Taglialatela, M., 2002. Benign familial neonatal convulsions caused by altered gating of KCNQ2/KCNQ3 potassium channels. J. Neurosci. 15; 22(2):RC199.

Cavaletti, G., Tredici, G., Petruccioli, M.G., Donde, E., Tredici, P., Marmiroli, P. et al., 2001. Effects of different schedules of oxaliplatin treatment on the peripheral nervous system of the rat. Eur. J. Cancer 37(18): 2457-2463.

Citi V., Martelli, A., Testai, L., Marino, A., Breschi, M.C., Calderone, V., 2014. Hydrogen sulfide releasing capacity of natural isothiocyanates: is it a reliable explanation for the multiple biological effects of Brassicaceae? Planta Med. 80: 610-613.

Di Cesare Mannelli, L., Maresca, M., Farina, C., Scherz, M.W., Ghelardini, C., 2015a. A model of neuropathic pain induced by sorafenib in the rat: Effect of dimiracetam. Neurotoxicology 50: 101-107.

Di Cesare Mannelli, L., Pacini, A., Corti, F., Boccella, S., Luongo, L., Esposito, E., Cuzzocrea, S., Maione, S., Calignano, A., Ghelardini, C., 2015b. Antineuropathic profile of N-palmitoylethanolamine in a rat model of oxaliplatin-induced neurotoxicity. PLoS One 10(6):e0128080. doi: 10.1371/journal.pone.0128080. eCollection 2015.

Di Cesare Mannelli, L., Pacini, A., Bonaccini, L., Zanardelli, M., Mello, T., Ghelardini, C., 2013. Morphologic features and glial activation in rat oxaliplatin-dependent neuropathic pain. J Pain 14(12): 1585-1600.

Distrutti, E., Sediari, L., Mencarelli, A., Renga, B., Orlandi, S., Antonelli, E. et al., 2006. Evidence that hydrogen sulfide exerts antinociceptive effects in the gastrointestinal tract by activating KATP channels. IPJ Pharmacol. Exp. Ther. 316(1): 325-35.

Dougherty, P.M., Cata, J.P., Cordella, J.V., Burton, A., Weng, H.R., 2004. Taxol-induced sensory disturbance is characterized by preferential impairment of myelinated fiber function in cancer patients. Pain 109: 32-42.

Du, X., Gamper, N., 2013. Potassium channels in peripheral pain pathways: expression, function and therapeutic potential. Curr. Neuropharmacol. 11(6):621-640.

Enokido, Y., Suzuki, E., Iwasawa, K., Namekata, K., Okazawa, H., Kimura, H., 2005. Cystathionine β-synthase, a key enzyme for homocysteine metabolism, is preferentially expressed in the radial glia/astrocyte lineage of developing mouse CNS. FASEB J. 19(13): 1854-1856.

Fariello, R.G., Ghelardini, C., Di Cesare Mannelli, L., Bonanno, G., Pittaluga, A., Milanese, M. et al., 2014. Broad spectrum and prolonged efficacy of dimiracetam in models of neuropathic pain. Neuropharmacology 81:85-94.

Gamper, N., Zaika, O., Li, Y., Martin, P., Hernandez, C.C., Perez, M.R., Wang, A.Y., Jaffe, D.B., Shapiro, M.S., 2006. Oxidative modification of M-type K(+) channels as a mechanism of cytoprotective neuronal silencing. EMBO J. 25:4996-5004.

Garcia Bereguiain, M.A., Samhan Arias, A.K., Martin Romero, F.J., Gutierrez-Merino, C., 2008. Hydrogen sulfide raises cytosolic calcium in neurons through activation of L-type Ca2+ channels. Antiox. Redox. Signal. 10(1): 31-42.

Hadley, J.K., Noda, M., Selyanko, A.A., Wood, I.C., Abogadie, F.C., Brown, D.A., 2000. Differential tetraethylammonium sensitivity of KCNQ1-4 potassium channels. Br. J. Pharmacol. 129(3): 413-415.

Hayashi, H., Iwata, M., Tsuchimori, N., Matsumoto, T., 2014. Activation of peripheral KCNQ channels attenuates inflammatory pain. Mol. Pain. 10: 15.

Hershman, D.L., Lacchetti, C., Dworkin, R.H., Smith, E.M.L., Bleeker, J., Cavaletti, G. et al., 2014. Prevention and management of chemotherapy-induced peripheral neuropathy in survivors of adult cancers: American Society of Clinical Oncology clinical practice guideline. J. Clin. Oncol. 32: 1941-1967.

Ito, S., Tajima, K., Nogawa, M., Inoue, N., Kyoi, T., Takahashi, Y., Sasagawa, T., Nakamura, A., Kotera, T., Ueda, M., Yamashita, Y., Banno, K., 2012. Etodolac, a cyclooxygenase-2 inhibitor, attenuates paclitaxel-induced peripheral neuropathy in a mousemodel of mechanical allodynia. J. Pharmacol. Exp. Ther. 342: 53-60.

Jiang, S.P., Zhang, Z.D., Kang, L.M., Wang, Q.H., Zhang, L., Chen, H.P., 2016. Celecoxib reverts oxaliplatin-induced neuropathic pain through inhibiting PI3K/Akt2 pathway in the mouse dorsal root ganglion. Exp. Neurol. 275: 11-16.

Kamat, P.K., Kalani, A., Tyagi, N., 2015. Role of hydrogen sulfide in brain synaptic remodeling. Methods Enzymol. 555: 207-29.

Kida, K., Marutani, E., Nguyen, R.K., Ichinose, F., 2015. Inhaled hydrogen sulfide prevents neuropathic pain after peripheral nerve injury in mice. Nitric Oxide 46: 87-92.

King, C.H., Scherer, S.S., 2012. Kv7.5 is the primary Kv7 subunit expressed in C-fibers. J. Comp. Neurol. 520: 1940-1950.

Lang, P.M., Fleckenstein, J., Passmore, G.M., Brown, D.A., Grafe, P., 2008. Retigabine reduces the excitability of unmyelinated peripheral human axons. Neuropharmacology 54(8):1271-1278.

Lee, S.W., Hu, Y.S., Hu, L.F., Lu, Q., Dawe, G.S., Moore, P.K. et al., 2006. Hydrogen sulphide regulates calcium homeostasis in microglial cells. Glia 54: 116–124.

Li, L., Whiteman, M., Guan, Y.Y., Neo, K.L., Cheng, Y., Lee, S.W. et al., 2008. Characterization of a novel, water-soluble hydrogen sulfide-releasing molecule (GYY4137): new insights into the biology of hydrogen sulfide. Circulation 117: 2351–2360.

Lin, J.Q., Luo, H.Q., Lin, C.Z., Chen, J.Z., Lin, X.Z., 2014. Sodium hydrosulfide relieves neuropathic pain in chronic constriction injured rats. Evid. Based. Complement. Alternat. Med. 2014: 514898.

Martelli, A., Testai, L., Breschi, M.C., Lawson, K., McKay, N.G., Miceli, F. et al. 2013a. Vasorelaxation by hydrogen sulphide involves activation of Kv 7 potassium channels. Pharmacol Res 70(1): 27-34.

Martelli, A., Testai, L., Citi, V., Marino, A., Pugliesi, I., Barresi, E. et al., 2013b. Arylthioamides as H_2S donors: l-cysteine-activated releasing properties and vascular effects in vitro and in vivo. ACS Med. Chem. Lett. 4(10): 904-908.

Martelli, A., Testai., L., Citi, V., Marino, A., Bellagambi, F.G., Ghimenti, S., et al., 2014. Pharmacological characterization of the vascular effects of aryl isothiocyanates: is hydrogen sulfide the real player? Vascul. Pharmacol. 60(1): 32-41.

Martire, M., Castaldo, P., D'Amico, M., Preziosi, P., Annunziato, L., Taglialatela, M., 2004. M channels containing KCNQ2 subunits modulate norepinephrine, aspartate, and GABA release from hippocampal nerve terminals. J. Neurosci. 24(3): 592-597.

McGrath, J.C., Lilley, E., 2015. Implementing guidelines on reporting research using animals (ARRIVE etc.): new requirements for publication in BJP. Br. J. Pharmacol. 172(13): 3189-3193.

Miceli, F., Soldovieri, M.V., Ambrosino, P., Barrese, V., Migliore, M., Cilio, M.R, et al., 2013. Genotype-phenotype correlations in neonatal epilepsies caused by mutations in the voltage sensor of K(v)7.2 potassium channel subunits. Proc. Natl. Acad. Sci. USA 110(11): 4386-4391.

Miceli, F., Soldovieri, M.V., Martire, M., Taglialatela, M., 2008. Molecular pharmacology and therapeutic potential of neuronal Kv7-modulating drugs. Curr. Opin. Pharmacol. 8(1): 65-74.

Nagpure, B.V., Bian, J.S., 2015. Brain, Learning, and Memory: Role of H_2S in Neurodegenerative Diseases. Handb. Exp. Pharmacol. 230: 193-215.

Nodera, H., Spieker, A., Sung, M., Rutkove, S., 2011. Neuroprotective effects of Kv7 channel agonist, retigabine, for cisplatin-induced peripheral neuropathy. Neurosci. Lett. 505(3): 223-7.

O'Callaghan, J.P., Holtzman, S.G., 1975. Quantification of the analgesic activity of narcotic antagonists by a modified hot-plate procedure. J. Pharmacol. Exp. Ther. 192:497-505.

Passmore, G.M., Selyanko, A.A., Mistry, M., Al-Qatari, M., Marsh, S.J., Matthews, E.A., et al., 2003. KCNQ/M currents in sensory neurons: significance for pain therapy. J Neurosci 23: 7227-7236.

Paul, B.D., Snyder, S.H., 2015. H_2S: A Novel Gasotransmitter that Signals by Sulfhydration. Trends Biochem. Sci. 40(11): 687-700.

Pietri, R., Román-Morales, E., López-Garriga, J., 2011. Hydrogen sulfide and hemeproteins: knowledge and mysteries. Antioxid. Redox. Signal. 15: 393-404.

Polomano, R.C., Mannes, A.J., Clark, U.S., Bennett, G.J., 2001. A painful peripheral neuropathy in the rat produced by the chemotherapeutic drug, paclitaxel. Pain 94(3): 293-304.

Rashid, M.H., Inoue, M., Toda, K., Ueda, H., 2004. Loss of peripheral morphine analgesia contributes to the reduced effectiveness of systemic morphine in neuropathic pain. J. Pharmacol. Exp. Ther. 309(1): 380-387.

Roediger, W.E., Moore, J., Babidge, W., 1997. Colonic sulfide in pathogenesis and treatment of ulcerative colitis. Dig. Dis. Sci. 42(8): 1571–1579.

Rose, K., Ooi, L., Dalle, C., Robertson, B., Wood, I.C., Gamper, N., 2011. Transcriptional repression of the M channel subunit Kv7.2 in chronic nerve injury. Pain 152: 742-754.

Schleifenbaum, J., Köhn, C., Voblova, N., Dubrovska, G., Zavarirskaya, O., Gloe, T. et al., 2010. Systemic peripheral artery relaxation by KCNQ channel openers and hydrogen sulfide. Journal of hypertension 28: 1875-1882.

Schwarz, J.R., Glassmeier, G., Cooper, E.C., Kao, T.C., Nodera, H., Tabuena, D. et al., 2006. KCNQ channels mediate I_{Ks}, a slow K^+ current regulating excitability in the rat node of Ranvier. J. Physiol. 573(Pt 1): 17-34.

Shibuya, N., Tanaka, M., Yoshida, M., Ogasawara, Y., Togawa, T., Ishii, K., et al., 2009. 3-Mercaptopyruvate sulfurtransferease produces hydrogen sulfide and bound sulfane sulfur in the brain. Antioxid. Redox. Signal. 11: 703–714.

Sittl, R., Carr, R.W., Fleckenstein, J., Grafe, P., 2010. Enhancement of axonal potassium conductance reduces nerve hyperexcitability in an in vitro model of oxaliplatin-induced acute neuropathy. Neurotoxicology 31: 694-700.

Soldovieri, M.V., Cilio, M.R., Miceli, F., Bellini, G., Miraglia del Giudice, E., Castaldo, P., Hernandez, C.C., Shapiro, M.S., Pascotto, A., Annunziato, L., Taglialatela, M., 2007. Atypical gating of M-type potassium channels conferred by mutations in uncharged residues in the S4 region of KCNQ2 causing benign familial neonatal convulsions. J. Neurosci. 27(18):4919-28.

Soldovieri, M.V., Miceli, F., Taglialatela, M., 2011. Driving with no brakes: molecular pathophysiology of Kv7 potassium channels. Physiology (Bethesda) 26(5): 365-376.

Souglakos, A.J., Mavroudis, D., Kakolyris, S., Kourousis, C.H., Vardakis, N., Androulakis, N. et al., 2002. Triplet combination with irinotecan plus oxaliplatin plus continuous-infusion fluorouracil and leucovorin as first-line treatment in metastatic colorectal cancer: a multicenter phase II trial. J. Clin. Oncol. 20: 2651-2657.

Szabó, C., 2007. Hydrogen sulphide and its therapeutic potential. Nat. Rev. Drug. Discov. 6: 917-935.

Szabo, C., Ransy, C., Módis, K., Andriamihaja, M., Murghes, B., Coletta, C., et al., 2014. Regulation of mitochondrial bioenergetic function by hydrogen sulfide. Part I. Biochemical and physiological mechanisms. Br. J. Pharmacol. 171:2099-2122.

Ta, L.E., Low, P.A., Windebank, A.J., 2009. Mice with cisplatin and oxaliplatin-induced painful neuropathy develop distinct early responses to thermal stimuli. Mol. Pain 5: 9.
Terada, Y., Kawabata, A., 2015. H_2S and Pain: A Novel Aspect for Processing of Somatic, Visceral and Neuropathic Pain Signals. Handb. Exp. Pharmacol. 230: 217-30.

Testai, L., Barrese, V., Soldovieri, M.V., Ambrosino, P., Martelli, A., Vinciguerra, I. et al., 2015. Expression and function of Kv7. 4 channels in Rat cardiac mitochondria: possible targets for cardioprotection. Cardiovasc. Res. 110(1): 40-50.

Wallace, J.L., Wang, R., 2015. Hydrogen sulfide-based therapeutics: exploiting a unique but ubiquitous gasotransmitter. Nat. Rev. Drug. Discov. 14(5): 329-345.

Wang, R., 2002. Two's company, three'sa crowd: can H_2S be the third endogenous gaseous transmitter? FASEB J. 16(13): 1792-1798.

Wang, J.J., Li, Y., 2016. KCNQ potassium channels in sensory system and neural circuits. Acta Pharmacol. Sin. 37(1): 25-33.

Wang, H.S., Pan, Z., Shi, W., Brown, B.S., Wymore, R.S., Cohen, I.S. et al., 1998. KCNQ2 and KCNQ3 potassium channel subunits: molecular correlates of the M-channel. Science 282(5395): 1890-1893.

Ward, S.J., McAllister, S.D., Kawamura, R., Murase, R., Neelakantan, H., Walker, E.A. 2014. Cannabidiol inhibits paclitaxel□induced neuropathic pain through 5-HT1A receptors without diminishing nervous system function or chemotherapy efficacy. Br. J. Pharmacol. 171: 636–645.

Xu, F., Xu, S., Wang, L., Chen, C., Zhou, X., Lu, Y., Zhang, H., 2011. Antinociceptive efficacy of verticinone in murine models of inflammatory pain and paclitaxel induced neuropathic pain. Biol. Pharm. Bull. 34:1377-82.

Zhao, Y., Biggs, T.D., Xian, M., 2014. Hydrogen sulfide (H_2S) releasing agents: chemistry and biological applications. Chem. Commun. 50: 11788-11805.

Zhao, H., Chan, S.J., Ng, Y.K., Wong, P.T.H., 2013. Brain 3-mercaptopyruvate sulfurtransferase (3MST): cellular localization and downregulation after acute stroke. PloS one 8(6): e67322.

Zheng, Q., Fang, D., Liu, M., Cai, J., Wan, Y., Han, J.S. et al., 2013. Suppression of KCNQ/M (Kv7) potassium channels in dorsal root ganglion neurons contributes to the development of bone cancer pain in a rat model. Pain 154(3): 434-48.

Zheng, Y., Ji, X., Ji, K., Wang, B., 2015. Hydrogen sulfide prodrugs—a review. Acta Pharmaceutica Sinica B 5(5): 367-377.

Figure captions

Figure 1. Effects of H_2S donors on paclitaxel-induced neuropathic pain. The response to a thermal stimulus was evaluated by the Cold plate test measuring the latency (s) to pain-related

behaviors (lifting or licking of the paw). Mice were treated with paclitaxel (2.0 mg kg^{-1} i.p.) on four alternate days (days 1, 3, 5 and 7) and the acute tests were performed on day 15. a) P-ITC, b) CP-ITC, and c) AITC (1.33, 4.43 and 13.31 μmol kg^{-1}) NaHS (4.43, 13.31 and 38 μmol kg^{-1}) were administered s.c.. Measurements were performed 15, 30, 45 and 60 min after injection. Control mice were treated with vehicle. Each value represents the mean of 16 mice per group, performed in 2 different experimental sets. *P<0.05 and **P<0.01 *vs* paclitaxel + vehicle treated animals.

Figure 2. Effects of H_2S donors on oxaliplatin-induced neuropathic pain. The response to a thermal stimulus was evaluated by the Cold plate test measuring the latency (s) to pain-related behaviors (lifting or licking of the paw). Mice were daily treated i.p. with oxaliplatin 2.4 mg kg^{-1}. Tests were performed on day 15. a) P-ITC, b) CP-ITC (both at 1.33, 4.43 and 13.31 μmol kg^{-1}), and c) NaHS (4.43, 13.31 and 38 μmol kg^{-1}) were administered s.c.. Measurements were performed 15, 30, 45 and 60 min after injection. The reference compounds d) morphine (21.75 μmol kg^{-1} s.c.), celecoxib (104.88 μmol kg^{-1} s.c.), duloxetine (50.43 μmol kg^{-1} p.o.) and pregabalin (94.20 μmol kg^{-1} p.o.) were administered, pain threshold was assessed 15, 30, 45 and 60 min after injection. Control mice were treated with vehicle. Each value represents the mean of 16 mice *per* group, performed in 2 different experimental sets. *P<0.05 and **P<0.01 *vs* oxaliplatin + vehicle treated mice.

Figure 3. Role of H_2S in the relief of oxaliplatin-induced neuropathic pain. The latency (s) to pain-related behaviors (lifting or licking of the paw) was measured by the Cold plate test. Mice were daily treated i.p. with oxaliplatin (2.4 mg kg^{-1}) and behavior was measured on day 15. a) A-ITC (1.33, 4.43 and 13.31 μmol kg^{-1} s.c.) was compared with A-IC (13.31 μmol kg^{-1} s.c.). b) NaHS (13.31 μmol kg^{-1} s.c.), P-ITC, CP-ITC, A-ITC and the morpholine derivative GYY4137 (GYY) (all at 4.43 μmol kg^{-1} s.c.) were administered alone or in mixture with Hb (3.10 μmol kg^{-1}). The histogram shows the average of resulting AUC. Control mice were treated with vehicle. Each value represents the mean of 16 mice *per* group, performed in 2 different experimental sets. *P<0.05 and **P<0.01 *vs* oxaliplatin + vehicle treated mice.

Figure 4. Involvement of Kv7 channels in H_2S-mediated anti-neuropathic effect. The latency (s) to pain-related behaviors (lifting or licking of the paw) was measured by the Cold plate test. Mice were daily treated i.p. with oxaliplatin (2.4 mg kg^{-1}) and behavior was measured on day 15. a) P-ITC, CP-ITC, A-ITC (4.43 μmol kg^{-1}) and NaHS (13.31 μmol kg^{-1}) were administered s.c.. XE991 (2.66 μmol kg^{-1}) was administered i.p. 15 min before H_2S-donors. The histograms show the

average of resulting AUC. b) Retigabine (2.66 μmol kg^{-1}) was administered p.o. in the absence and in the presence of a pretreatment (15 min before) with XE991 (2.66 μmol kg^{-1} i.p). c) P-ITC (4.43 μmol/mouse) and NaHS (13.31 μmol/mouse) were administered i.c.v. in the absence and in the presence of a pretreatment (15 min before) with XE991 (2.66 μmol kg^{-1} i.p.). Control mice were treated with vehicle. Each value represents the mean of 16 mice *per* group, performed in 2 different experimental sets. *P<0.05 and **P<0.01 *vs* oxaliplatin + vehicle treated mice.

Figure 5. Effect of H_2S donors on Kv7.2/3 currents heterologously-expressed in CHO cells. a) Macroscopic currents recorded in response to a voltage ramp from -80 to 0 mM in CHO cells expressing Kv7.2/7.3 channels in control solution (CTL) or after perfusion with the maximal concentration tested of each of the following compound (in mM): 0.01 retigabine (RTG), 10 NaHS (NaHS), 10 allyl-isocyanate (A-IC), 10 allyl-isothiocyanate (A-ITC), 100 phenyl-isothiocyanate (P-ITC), or 10 3-carboxyphenyl-isothiocyanate (CP-ITC), as indicated. Current scale: 200 pA; time scale: 200 ms. b and c) Quantification of the effects prompted by each compound on peak current increase (b) or ΔV_{-40} (c). Single asterisks indicate, for each drug, values significantly (P<0.05) different versus controls; double and triple asterisks indicate values significantly different (P<0.05) versus controls and versus values recorded upon perfusion of a lower drug concentration. The numbers on top of each bar indicate the number of measurements, each from a different cell.

Supplementary material

Supplementary Figure legends

Supplementary Figure S1. Effects of H_2S donors on paclitaxel-induced neuropathic pain. The response to a mechanical stimulus was evaluated by the Von Frey test measuring the withdrawal threshold (g). Mice were treated with paclitaxel (2.0 mg kg^{-1} i.p.) on four alternate days (days 1, 3, 5 and 7) and the acute tests were performed on day 15. P-ITC (4.43 μmol kg^{-1}), CP-ITC (4.43 μmol kg^{-1}), and NaHS (13.31 μmol kg^{-1}) were administered s.c.. Measurements were performed 15, 30, 45 and 60 min after injection. Control mice were treated with vehicle. Each value represents the mean of 12 mice per group, performed in 2 different experimental sets. *P<0.05 and **P<0.01 *vs* paclitaxel + vehicle treated animals.

Supplementary Figure S2. Effects of H_2S donors on oxaliplatin-induced neuropathic pain. The response to a mechanical stimulus was evaluated by the Von Frey test measuring the withdrawal threshold (g). Mice were daily treated i.p. with oxaliplatin 2.4 mg kg^{-1}. Tests were performed on day 15. P-ITC (4.43 μmol kg^{-1}), CP-ITC (4.43 μmol kg^{-1}), and NaHS (13.31 μmol kg^{-1}) were administered s.c.. Measurements were performed 15, 30, 45 and 60 min after injection. Control mice were treated with vehicle. Each value represents the mean of 12 mice *per* group, performed in 2 different experimental sets. *P<0.05 and **P<0.01 *vs* oxaliplatin + vehicle treated mice.

Supplementary Figure S3. Role of H_2S in the relief of oxaliplatin-induced neuropathic pain. The latency (s) to pain-related behaviors (lifting or licking of the paw) was measured by the Cold plate test. Mice were daily treated i.p. with oxaliplatin (2.4 mg kg^{-1}) and behavior was measured on day 15. Effect of the morpholine-derivative GYY4137 (4.43 μmol kg^{-1} s.c.) administered alone or in mixture with Hb (3.10 μmol kg^{-1}). Control mice were treated with vehicle. Each value represents the mean of 16 mice *per* group, performed in 2 different experimental sets. *P<0.05 and **P<0.01 *vs* oxaliplatin + vehicle treated mice.

Supplementary Figure S4. Effects of XE991 on oxaliplatin-induced neuropathic pain. The latency (s) to pain-related behaviors (lifting or licking of the paw) was measured by the Cold plate test. Mice were daily treated i.p. with oxaliplatin (2.4 mg kg^{-1}) and behavior was measured on day 15. Effects of XE991 (2.66, 7.98 and 26.60 μmol kg^{-1}) after administered i.p. administration. Control mice were treated with vehicle. Each value represents the mean of 10 mice *per* group, performed in 2 different experimental sets.

Supplementary Figure S5. Effects of H_2S donors on normal pain threshold. Compounds (NaHS, A-ITC and P-ITC) were injected s.c. Pain-related behavior (i.e. lifting and licking of the hind paw) were observed in the Hot Plate test, the time (s) of the first sign was recorded. Measurements were performed before and after treatments over time. Each value represents the mean of 10 mice *per* group, performed in 2 different experimental sets.

Supplementary Figure S6. Effect of CP-ITC on activation and deactivation kinetics of Kv7.2/3 currents expressed in CHO cells. a) Superimposed macroscopic Kv7.2/3 current traces recorded in response to the indicated voltage protocol in control solution (black trace) or after perfusion with 1 mM CP-ITC (gray trace). b) Kv7.2/3 current activation time constants (τ_f, empty symbols; τ_s, filled symbols) recorded in control solution (CTL, circles) or upon perfusion with 1 mM CP-ITC (CP-ITC, squares). c) Relative amplitudes of the fast (A_f) and slow (A_s) current activation components, expressed as A_f/A_f+A_s, recorded in control solution (circles) or upon perfusion with 1 mM CP-ITC (squares). Asterisks denote values significantly different from the corresponding control values ($p<0.05$). d) Superimposed macroscopic Kv7.2/3 current traces recorded in response to the indicated voltage protocol in control solution (CTL, black trace) or after perfusion with 1 mM CP-ITC (CP-ITC, gray trace). e) Deactivation time constants (τ) measured in control solution (circles) or upon perfusion with 1 mM CP-ITC (squares). Asterisks denote values significantly different from the corresponding control values ($P<0.05$).

Supplementary Figure S7. Effect of H_2S donors on Kv7.2 currents heterologously-expressed in CHO cells. a) Macroscopic currents recorded in response to a voltage ramp from -80 to 0 mM in CHO cells expressing Kv7.2 channels in control solution (CTL) or after perfusion with (in mM) 0.01retigabine (RTG), 1 NaHS, 1 A-ITC, or 1 CP-ITC, as indicated. Current scale: 100 pA; time scale: 200 ms. b and c) Quantification of the effects of each compound on maximal current density (b; data are expressed as % of controls, measured before drug exposure) or as ΔV_{-40} (c; data are expressed in mV). Single asterisks indicate values significantly different ($P<0.05$) versus controls; double asterisks indicates values significantly different ($P<0.05$) versus both control and the reference compound NaHS. In b), the numbers on top of each bar indicate the number of measurements, each from a different cell.

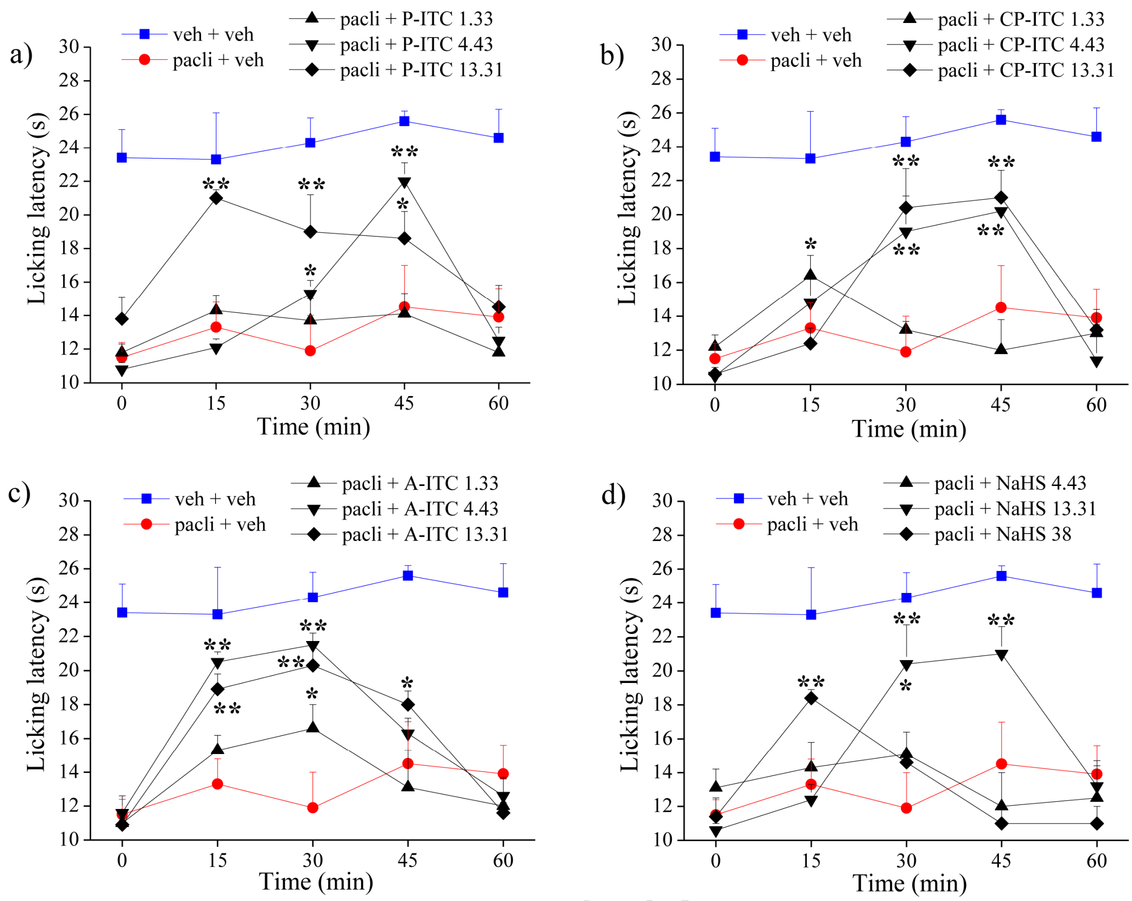

a)
veh + veh
pacli + veh
pacli + P-ITC 1.33
pacli + P-ITC 4.43
pacli + P-ITC 13.31
Licking latency (s)
Time (min)
b)
pacli + CP-ITC 1.33
pacli + CP-ITC 4.43
pacli + CP-ITC 13.31
c)
pacli + A-ITC 1.33
pacli + A-ITC 4.43
pacli + A-ITC 13.31
d)
pacli + NaHS 4.43
pacli + NaHS 13.31
pacli + NaHS 38

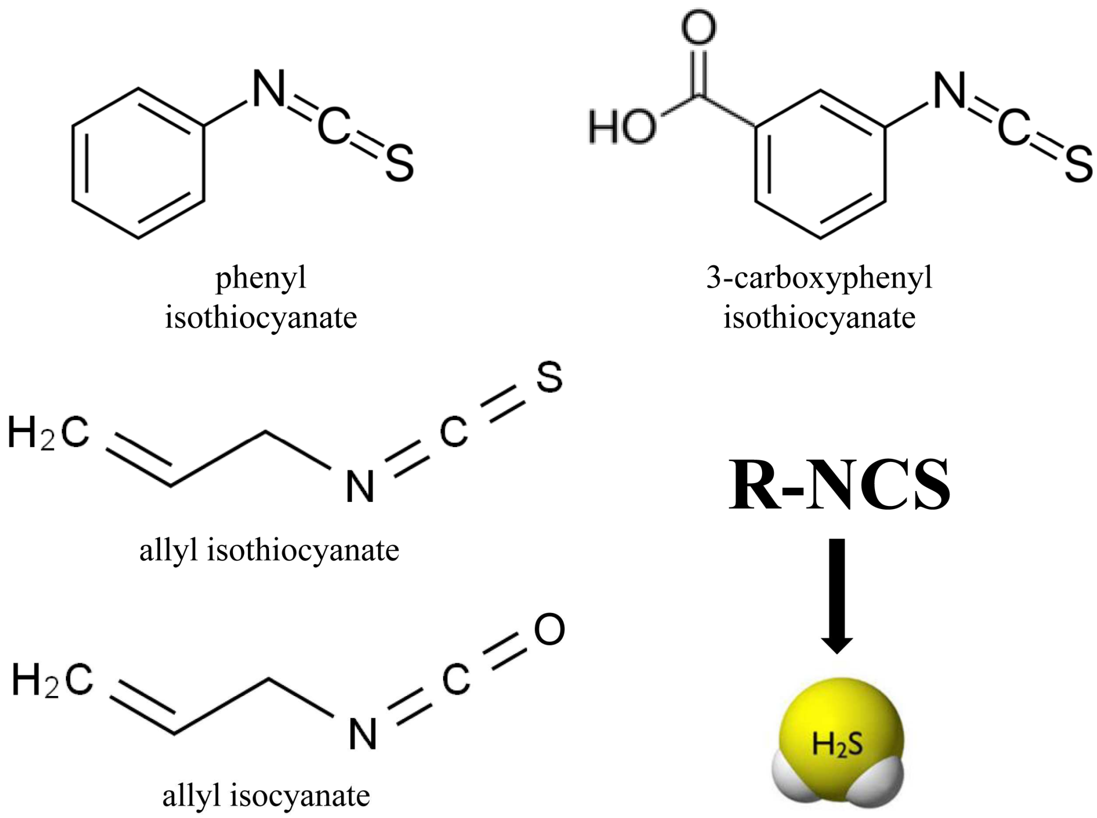
phenyl isothiocyanate
3-carboxyphenyl isothiocyanate
allyl isothiocyanate
allyl isocyanate
R-NCS
H2S

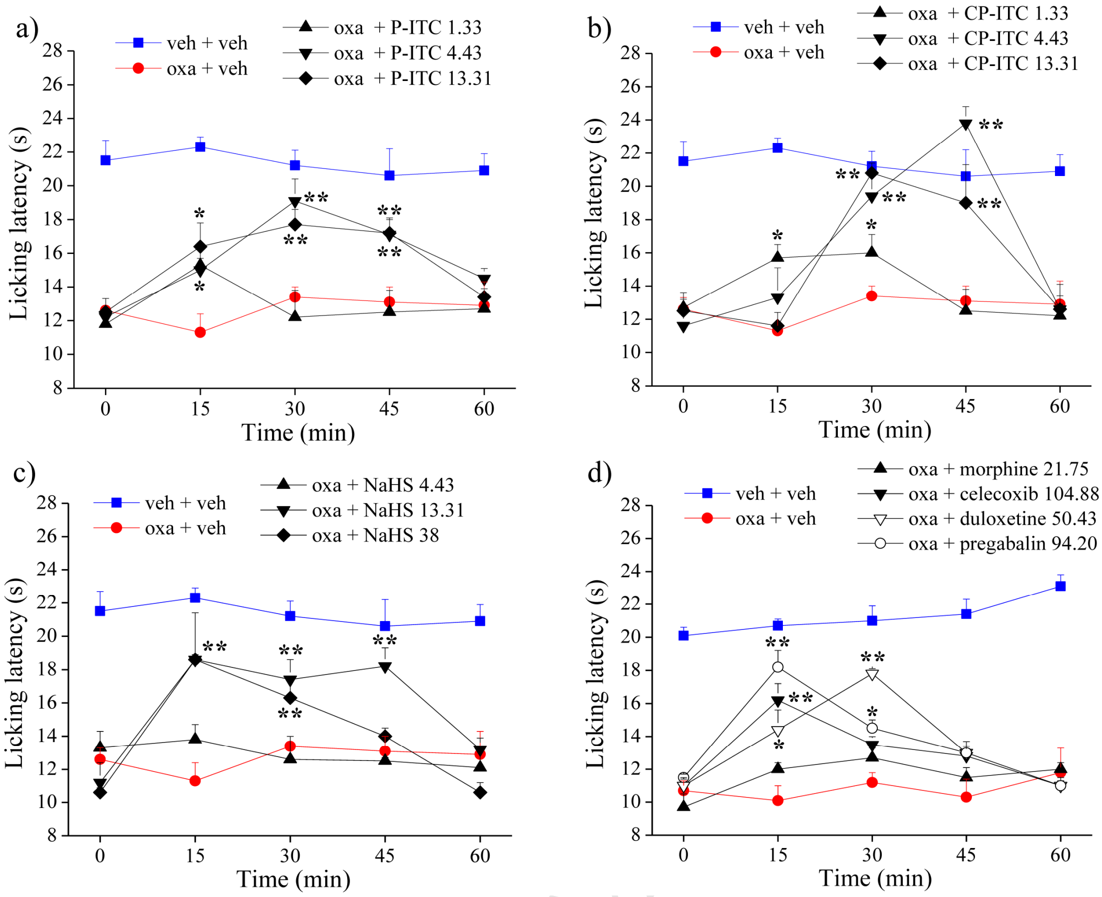
a)
veh + veh
oxa + veh
oxa + P-ITC 1.33
oxa + P-ITC 4.43
oxa + P-ITC 13.31
Licking latency (s)
Time (min)
b)
veh + veh
oxa + veh
oxa + CP-ITC 1.33
oxa + CP-ITC 4.43
oxa + CP-ITC 13.31
Licking latency (s)
Time (min)
c)
veh + veh
oxa + veh
oxa + NaHS 4.43
oxa + NaHS 13.31
oxa + NaHS 38
Licking latency (s)
Time (min)
d)
veh + veh
oxa + veh
oxa + morphine 21.75
oxa + celecoxib 104.88
oxa + duloxetine 50.43
oxa + pregabalin 94.20
Licking latency (s)
Time (min)

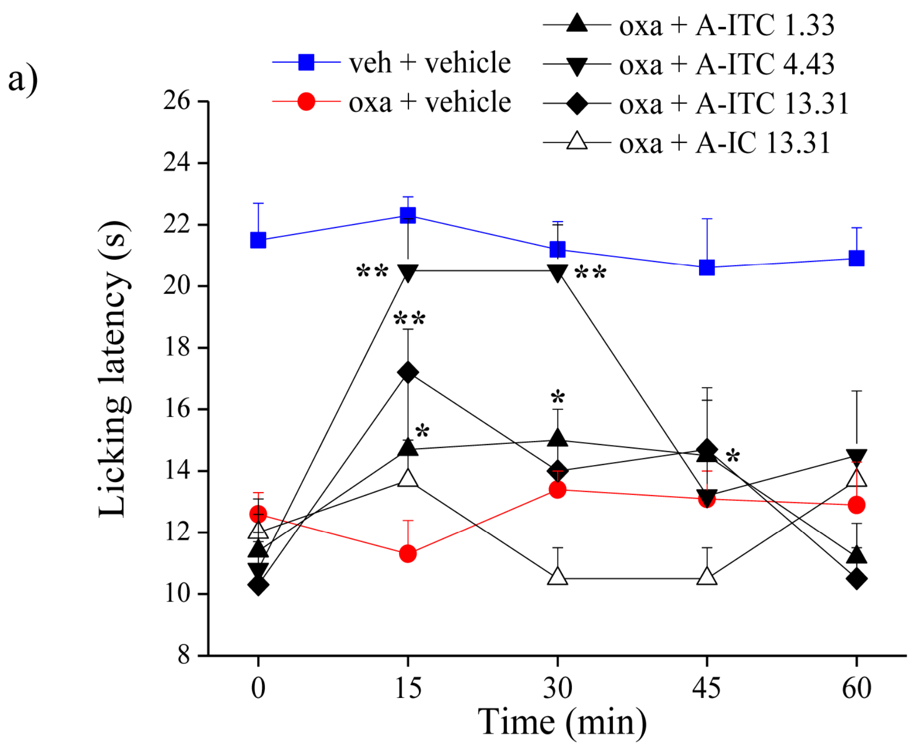
a)
veh + vehicle
oxa + vehicle
oxa + A-ITC 1.33
oxa + A-ITC 4.43
oxa + A-ITC 13.31
oxa + A-IC 13.31
Licking latency (s)
Time (min)
0
15
30
45
60
8
10
12
14
16
18
20
22
24
26
**
**
**
*
*
*

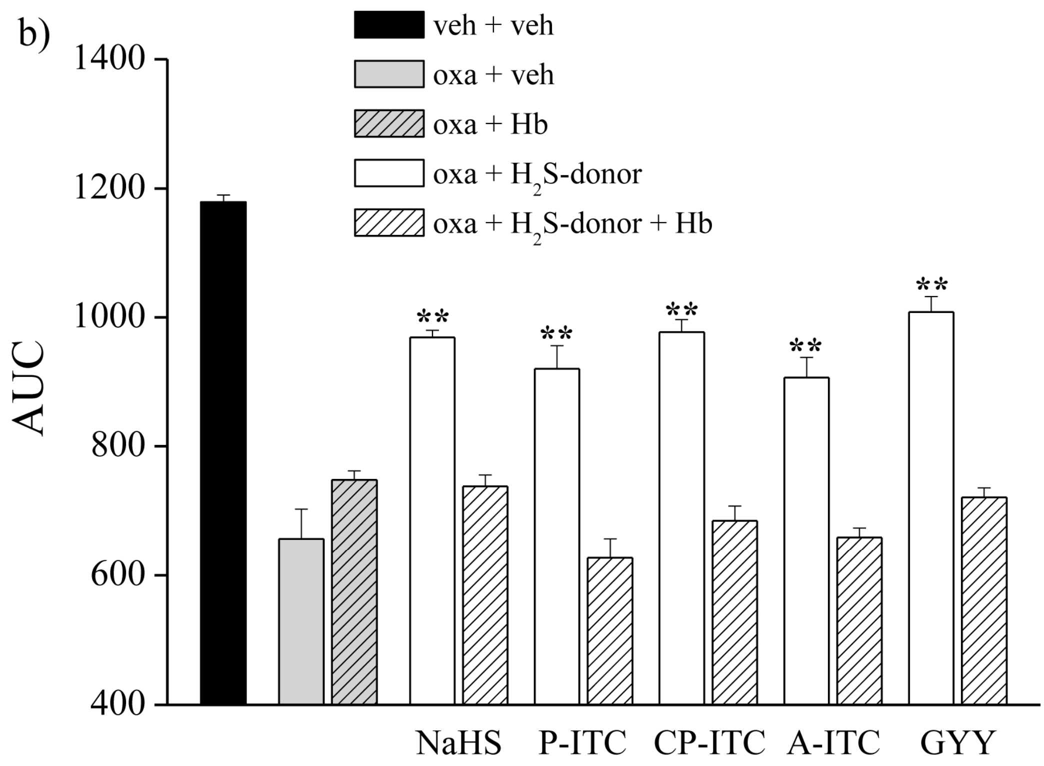
b)
veh + veh
oxa + veh
oxa + Hb
oxa + H2S-donor
oxa + H2S-donor + Hb
AUC
400
600
800
1000
1200
1400
**
**
**
**
**
NaHS
P-ITC
CP-ITC
A-ITC
GYY

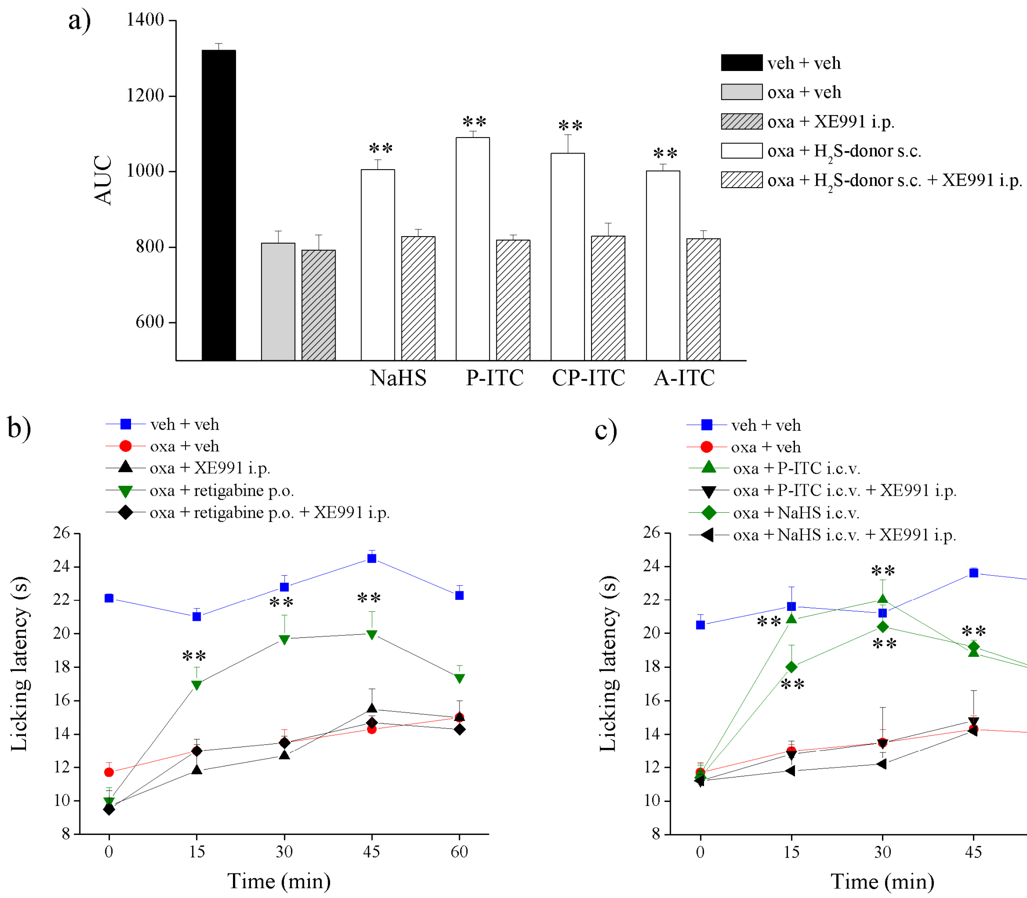
a)
AUC
1400
1200
1000
800
600
veh + veh
oxa + veh
oxa + XE991 i.p.
oxa + H2S-donor s.c.
oxa + H2S-donor s.c. + XE991 i.p.
**
NaHS
P-ITC
CP-ITC
A-ITC
b)
veh + veh
oxa + veh
oxa + XE991 i.p.
oxa + retigabine p.o.
oxa + retigabine p.o. + XE991 i.p.
Licking latency (s)
Time (min)
0
15
30
45
60
c)
veh + veh
oxa + veh
oxa + P-ITC i.c.v.
oxa + P-ITC i.c.v. + XE991 i.p.
oxa + NaHS i.c.v.
oxa + NaHS i.c.v. + XE991 i.p.
Licking latency (s)
Time (min)

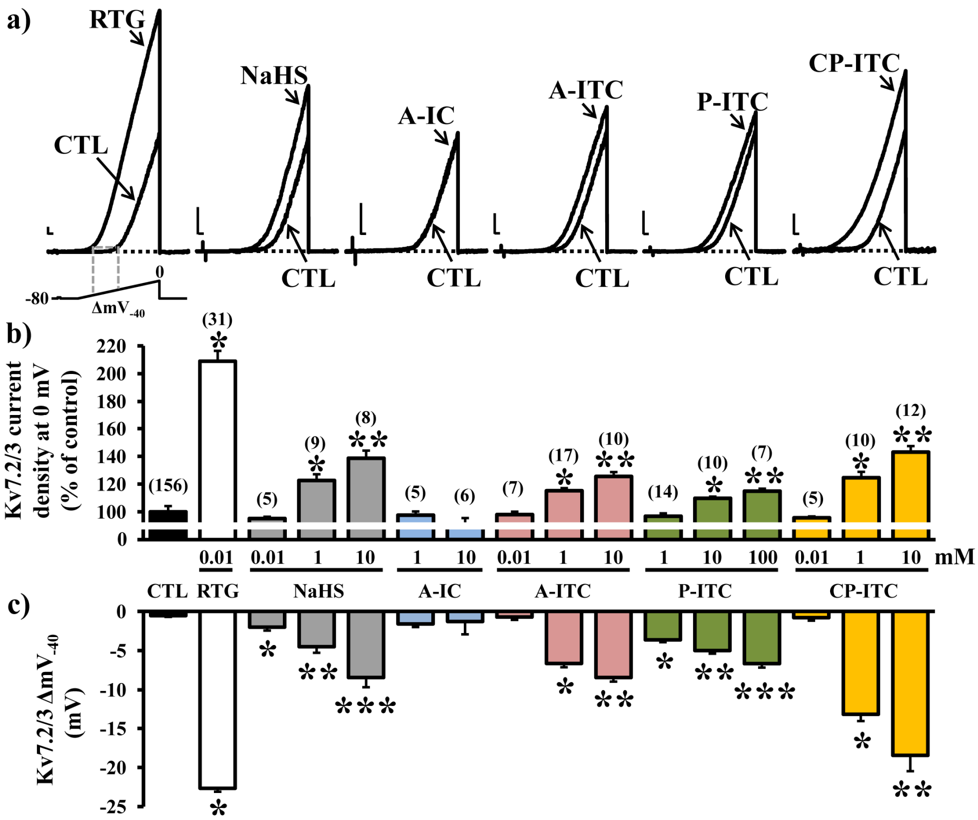
a)
RTG
CTL
NaHS
A-IC
A-ITC
P-ITC
CP-ITC
CTL
-80
0
ΔmV-40
b)
Kv7.2/3 current density at 0 mV (% of control)
0
100
120
140
160
180
200
220
(156)
(31)
(5)
(9)
(8)
(5)
(6)
(7)
(17)
(10)
(14)
(10)
(7)
(5)
(10)
(12)
0.01
0.01
1
10
1
10
0.01
1
10
1
10
100
0.01
1
10
mM
CTL
RTG
NaHS
A-IC
A-ITC
P-ITC
CP-ITC
c)
Kv7.2/3 ΔmV-40 (mV)
0
-5
-10
-15
-20
-25

- Natural and synthetic isothiocyanates reduce oxaliplatin-dependent neuropathic pain
- The efficacy is related to the property of releasing the gasotransmitter H_2S
- The pain relieving effect is reverted by the Kv7 potassium channel blocker XE991
- H_2S-releasing isothiocyanates potentiate Kv7.2/3 currents